

# Maximising the Value of Geophysical Data for Mineral Exploration: A Case Study from the Yilgarn Craton

**Mosayeb Khademi**

UniSA and MinEx CRC

[Mosayeb.khademi\\_zahedi@mymail.unisa.edu.au](mailto:Mosayeb.khademi_zahedi@mymail.unisa.edu.au)

**David Giles**

UniSA and MinEx CRC

[David.Giles@unisa.edu.au](mailto:David.Giles@unisa.edu.au)

**Vitaliy Ogarko**

UWA and MinEx CRC

[Vitaliy.ogarko@uwa.edu.au](mailto:Vitaliy.ogarko@uwa.edu.au)

**Mark Lindsay**

CSIRO and MinEx CRC

[Mark.Lindsay@csiro.au](mailto:Mark.Lindsay@csiro.au)

**Andrej Bona**

MinEx CRC

[A.Bona@curtin.edu.au](mailto:A.Bona@curtin.edu.au)

**Caroline Tiddy**

UniSA and MinEx CRC

[Caroline.Tiddy@unisa.edu.au](mailto:Caroline.Tiddy@unisa.edu.au)

## SUMMARY

Substantial investments are made in acquiring information for mineral exploration. However, quantifying critical data and developing an integrated workflow remains challenging. This study addresses these issues through a case study in the Yilgarn Craton, focusing on the Fortitude North prospect.

In poorly outcropping regions, potential field geophysics are crucial for targeting drill holes in gold exploration, however, they typically do not directly image gold deposits. Any relationship between gold deposits and these datasets must involve other elements of the mineral system. We use a mineral system model based on Yilgarn Craton orogenic gold deposits which identifies iron-rich mafic hosts with magmatic magnetite as favourable sites for gold deposition.

We performed gravity and magnetic inversions for the Laverton Tectonic Zone, mapping density and susceptibility ranges characteristic of doleritic host rocks containing magmatic magnetite. Areas matching these parameters constitute 14% of the total area and contains ~70% of known gold endowment. Sunrise Dam is excluded due to poor gravity data coverage, but its inclusion would potentially increase the contained endowment to ~90%.

We tested various area reduction strategies in a ~465 km<sup>2</sup> area around the Fortitude North prospect. Drilling the entire area to find a ~1Moz deposit is risky and expensive (100's M\$). Applying the same density and susceptibility filter used for the Laverton Tectonic Zone reduced the search area by 81%. This could be further refined using ground magnetics for targeting drilling in areas where favourable hosts are cross-cut by structures (demagnetised zones). During this talk, we will present a scenario where our approach reduces the search space to 5%. We propose collecting 3D seismic (~millions \$) to further target drilling (10's M\$) in a cost-effective manner. This demonstrates a quantitative example of the value of regional geophysical data combined with simple mineral systems models in mineral exploration.

**Key words:** Value of Information, Mineral Exploration, Orogenic gold, Geophysical Inversions, Yilgarn Craton.

## INTRODUCTION

Mineral deposits represent highly concentrated geochemical anomalies within Earth's crust, often localized in specific, small-volume segments. Despite the endowment richness of regions such as the Yilgarn Craton in Western Australia—one of the world's premier gold mining regions (Groves et al., 2003; Korsch & Doublier, 2016; Phillips et al., 2019)—locating new deposits remains a "needle-in-a-haystack" challenge due to the vast search area as the known gold endowment occupies a mere fraction of the upper kilometre of the crust in the Yilgarn Craton, representing the effective volume available for exploration within this region.

To address these challenges, mineral exploration campaigns commonly employ a volume-reduction strategy. This approach integrates a comprehensive understanding of the target mineral system, conceptualised through a mineral systems model, with strategic and scale-appropriate data acquisition (Hronsky & Kreuzer, 2019; McCuaig & Hronsky, 2014; Yousefi et al., 2021). Geophysical techniques are crucial in reducing the search volume for mineral deposits. In particular, potential field methods enable the visualisation, mapping, and interpretation of subtle geological features within the subsurface (Blaikie et al., 2013; Dentith & Mudge, 2014). Additionally, the distribution of physical properties, such as density and magnetic susceptibility, can be inferred through geophysical inversion.

This study presents a methodology for volume-reduction decisions in mineral exploration, applied to an Archaean orogenic gold system within the Laverton Tectonic Zone, part of the Eastern Goldfields Superterrane (EGS) in the Yilgarn Craton, Western Australia. The workflow quantifies uncertainty by utilising multiple inversions with a variety of realistic input parameters. The study area includes significant known gold deposits, such as Sunrise Dam and Granny Smith, two of the most major gold deposits in Western Australia, as well as numerous undeveloped prospects including the Fortitude North prospect (Fig. 1). The Fortitude North prospect is used as a case study due to its representation of Archaean orogenic gold prospectivity and the availability of relevant data for this study.

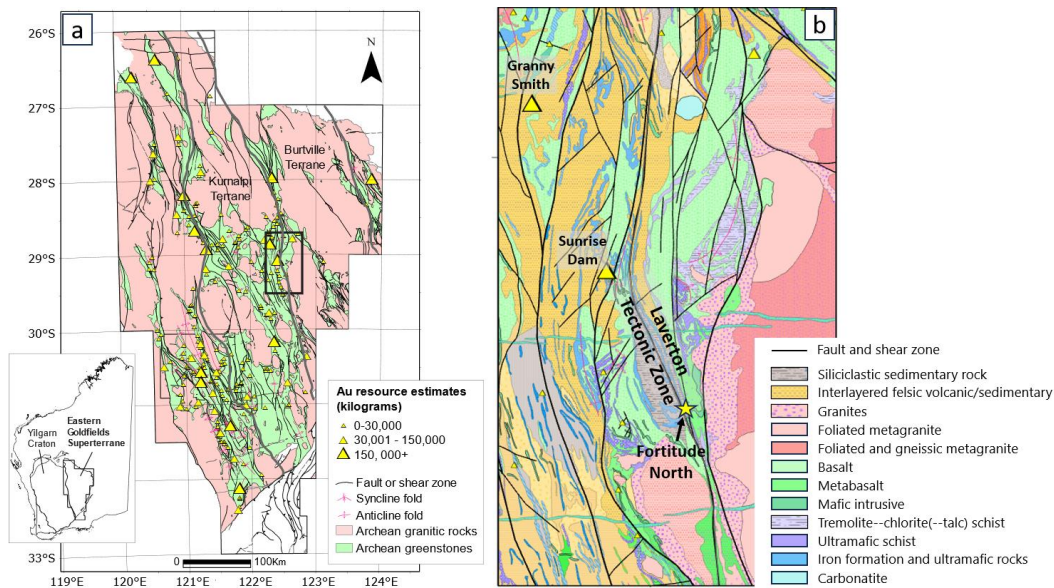


**Figure 1. a) Eastern Goldfields Superterrane, Yilgarn Craton, Western Australia (modified from 1:2.5M GSWA 2015 bedrock geology and crustal boundaries). The black box indicates the area shown in (b). b) Laverton Tectonic Zone with interpreted geology and structures, highlighting key gold deposits including Sunrise Dam, Granny Smith, and the Fortitude North prospect (modified from 1:500k GSWA 2020 data).**

In this analysis, geophysical inversions were performed on precompetitive gravity and aeromagnetic data to model density and magnetic susceptibility distributions at the camp scale. These distributions were correlated with geological features in a mineral systems model, focusing on magnetite-bearing dolerites, which are favourable for gold mineralisation where faulted and sheared (Hayman et al., 2021; Phillips et al., 1996). The area-reduction strategy was assessed using capture-efficiency plots (Baddeley et al., 2021; Porwal et al., 2010a) to evaluate known gold endowment within the Laverton Tectonic Zone.

The results of this case study highlight the value of precompetitive geophysical datasets in mineral exploration, with a focus on collecting petrophysical data from all components of the mineral system. These data provide critical constraints on geophysical modelling and inversion. The proposed workflow offers a systematic approach for reducing the search space, adaptable to various exploration scenarios, and helps guide the selection of the most appropriate and cost-effective exploration techniques at different scales.

## GEOPHYSICAL AND PETROPHYSICAL DATA COLLECTION AND PROCESSING

In this study, precompetitive regional gravity and aeromagnetic datasets were utilised to model subsurface density and magnetic susceptibility in the Laverton Tectonic Zone. The gravity data was sourced from the Geoscience Australia database, with 3470 gravity measurements covering the study area. The measurements were taken at an average station spacing of 1 km, with additional infill points at ~500 m spacing. In certain areas, data density is lower, with station spacing extending up to 4 kilometres. Aeromagnetic data were also sourced from the Geoscience Australia database (surveys P580 and P587). The P580 survey, conducted in 1989, consisted of east-west flight lines with a spacing of 400 m and a flight height of 100 m. The P587 survey, conducted in 1992, followed a similar pattern and flight lines spacing but flown at 60 m.

To minimise the background or regional response from the data, high-pass filtering was applied to both gravity and magnetic datasets. This process removed the long-wavelength regional signal, allowing the detection of shorter-wavelength anomalies associated with local geological responses related to shallow mineralised zones in the datasets, which are of primary interest in mineral exploration (Fig. 2). The filtered data was gridded at 500 m cell spacing for gravity and 250 m for magnetic data to improve data continuity. The processed datasets served as the input for geophysical inversions, which aimed to model the spatial distribution of density and magnetic susceptibility. These models were then correlated with geological features of the mineral systems model utilised for this analysis, focusing on magnetite-bearing dolerites, which can form favourable sites for gold deposition when faulted or sheared.

Along with geophysical data, bulk density and magnetic susceptibility measurements were collected from three drill holes at the Fortitude North prospect (19FNDD001, 20FNDD006 & 20FNDD008 – Fig. 3). Bulk density measurements at the Fortitude North prospect show doleritic host rocks have densities between 2.3 and 3.1 g/cm<sup>3</sup>, with modes around 2.85 and 3.00 g/cm<sup>3</sup>. Magnetic susceptibility in dolerites ranges from -1.77 to 1.95 log<sub>10</sub> × 10<sup>-3</sup> SI units, with a mode at -0.2 log<sub>10</sub> SI and elevated values between 0.8 and 1.95 log<sub>10</sub> × 10<sup>-3</sup> SI. The higher magnetic susceptibility in differentiated dolerites is linked to a magnetite-rich interval, likely affecting geophysical data.

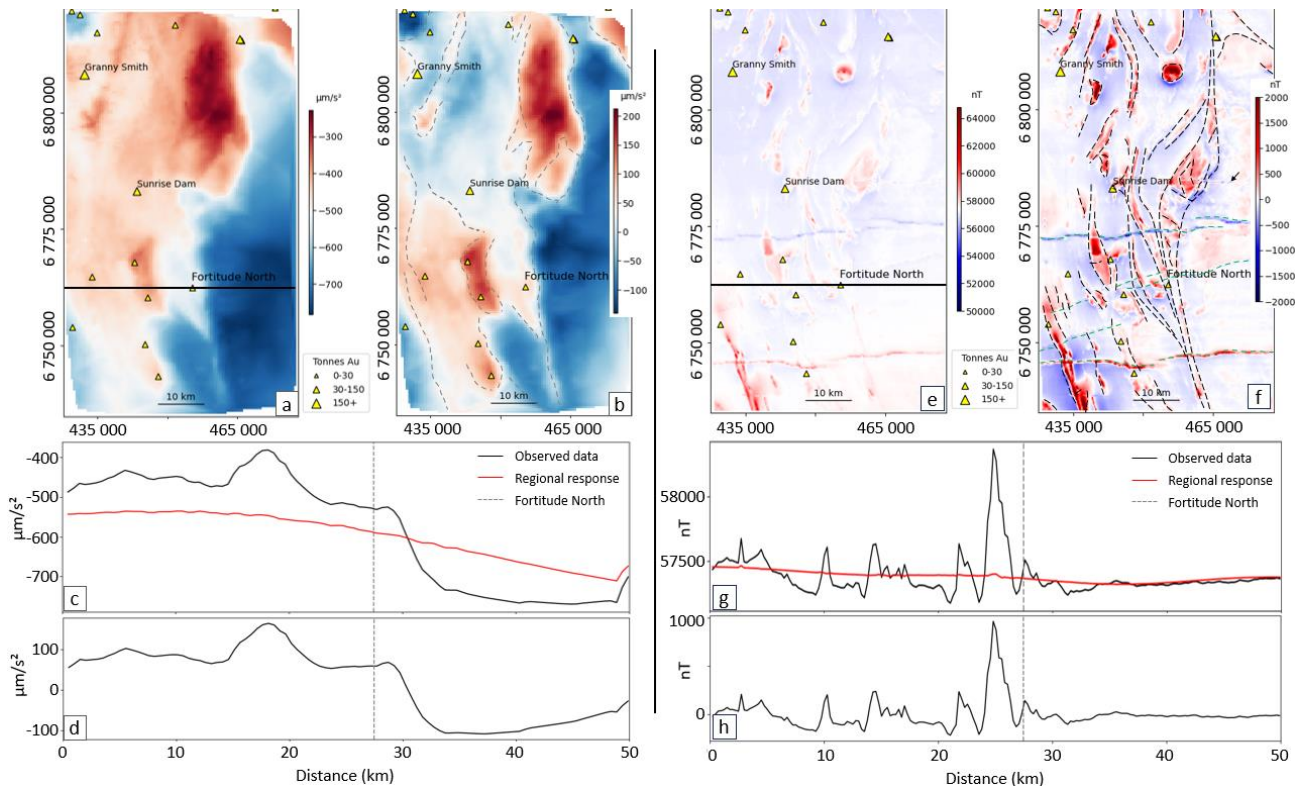


**Figure 2.** Gravity data before (a) and after (b) high-pass filtering, with regional trends indicated by dashed lines. Panels (c) and (d) show gravity profile traversing the Fortitude North prospect before and after filtering. Aeromagnetic maps are shown before (e) and after (f) high-pass filtering (dashed lines highlight patterns associated with greenstone belts and crosscutting features). Panel (g) shows the aeromagnetic profile without filtering, and panel (h) the post-filtered profile across the same traverse. The black lines in (a) and (e) indicate the profile locations. Location of maps is shown in Figure 1a.

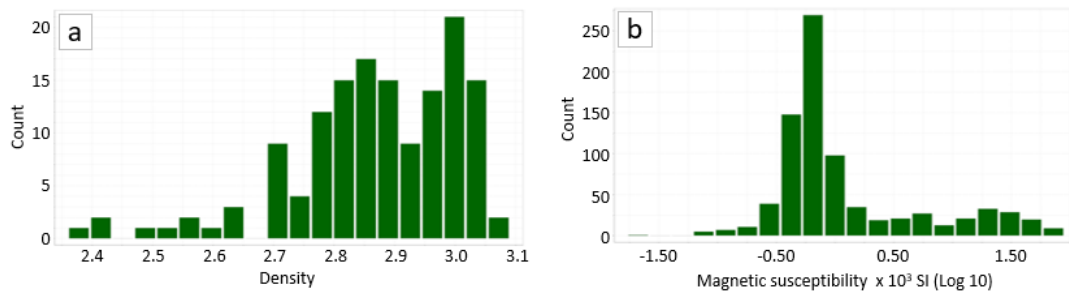


**Figure 3.** Histograms showing (a) bulk density; and (b) magnetic properties in differentiated dolerites. Data collected from drill holes 19FNDD001, 20FNDD006 and 20FNDD008.

## GEOPHYSICAL INVERSION

Geophysical inversion was a key part of this study, with the goal of estimating the 3D distribution of density and magnetic susceptibility across the study area. Using the Tomofast-x 3D inversion code developed by Giraud et al. (2021) and Ogarko et al. (2024), both gravity and aeromagnetic data were inverted to depths of 15 km and 5 km, respectively, to resolve subsurface density and magnetic susceptibility variations. Prior to running inversions, simulated in-filling of measurement points was performed using random sampling and down sampling to evaluate the effect of data density on inversion model performance. For gravity data, five ensembles were created, consisting of 300, 600, 1000, 1500, and 3000 measurement points (Fig. 4a–e). For aeromagnetic data, simulated in-filling was achieved by reducing the flight line spacing from 3200 m to 400 m in three successive steps (Fig. 4f–i). To account for variability within the data, 50 different datasets were generated for each sample size in both the gravity and aeromagnetic datasets. This was achieved by applying random sampling to the gravity data and down sampling to the aeromagnetic data. Gravity measurements were gridded into 500 m cells, while aeromagnetic data were gridded into 250 m cells for each sample size, ensuring a regular spatial distribution of measurements. The rationale for employing random sampling and down sampling techniques in this study was to evaluate the impact of data density and measurement locations on the inversion model's performance.



Inversions were then run using each of the subsampled gravity and aeromagnetic datasets. The mean and standard deviation of density and magnetic susceptibility estimates were calculated from the resulting ensemble of models. With 300 gravity measurement points ( $\sim 0.07$  stations per  $\text{km}^2$ ), the model shows diffuse positive density anomalies with poorly defined boundaries (Fig. 5a). As the number of points increases to 600 and 1000 ( $\sim 0.1$  and  $\sim 0.2$  stations per  $\text{km}^2$ ), some anomalies become slightly more defined, but they remain scattered and vague (Fig. 5b, c). Using 1500 points ( $\sim 0.3$  stations per  $\text{km}^2$ ), the high and low-density regions become more pronounced (e.g., the high-density region indicated by the black arrow in Figure 5), exhibiting linear trends that align with known geological structures, such as greenstone belts (Fig. 5d). The model based on 3000 points ( $\sim 0.7$  stations per  $\text{km}^2$ ) further refines these patterns, providing well-delineated density contrasts and confirming the distinct linear anomalies observed in previous runs (Fig. 5e). The inversion model derived from the complete dataset of 3470 measurement points ( $\sim 0.8$  stations per  $\text{km}^2$ ) is illustrated in Figure 5f. This model further confirms the linear to sub-linear patterns observed in the 1500- and 3000-point models. The standard deviation maps (Fig. 5, bottom row) show high variability co-located with positive gravity anomalies, indicating higher uncertainty in these regions. As the number of measurement points increases from 300 to 3000, high-variability areas become more localised and less pronounced. For example, high standard deviation near the Fortitude North prospect decreases with increasing measurement points, becoming minimal by the time 3000 points are used.

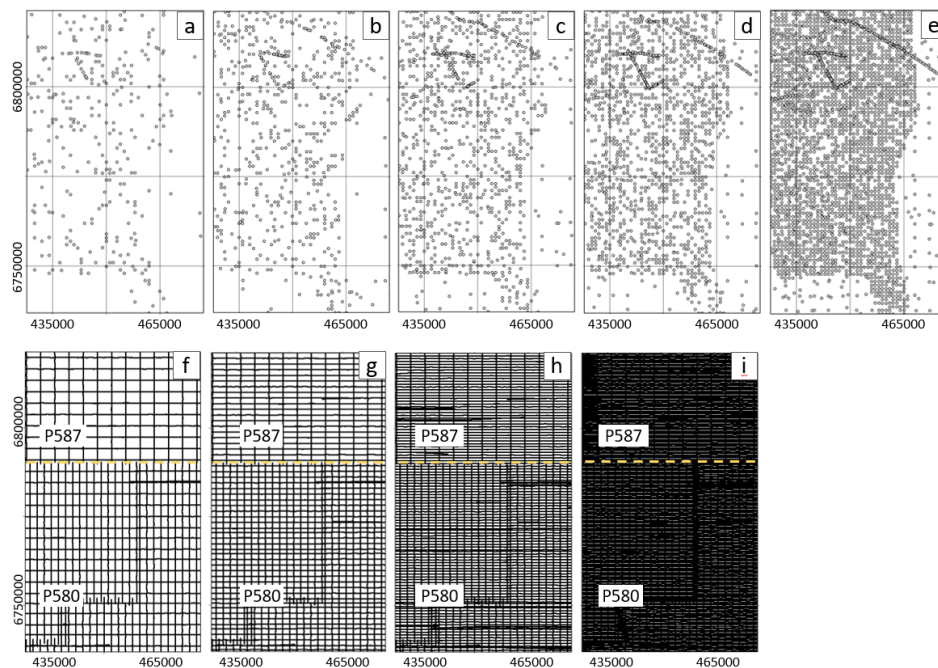


**Figure 4. Spatial distribution of gravity stations and aeromagnetic data at various sampling and line spacing levels. For gravity measurements: (a) 300 points, (b) simulated in-filled to 600, (c) 1000, (d) 1500, and (e) 3000 points. For aeromagnetic flight lines: (f) initial 3200 m line spacing, (g) simulated in-filled to 1600 m, (h) 800 m, and (i) 400 m. These are examples of each sample size amongst 49 other datasets.**

The inversion results from 3200 m line spacing aeromagnetic data show minimal variation with diffused anomalies and prominent North-South flight lines artefacts. The large black arrow in Figure 6a indicates a linear diffuse positive anomaly which is broad and lacks clear definition. Similarly, the standard deviation map indicates relatively high values associated with this linear anomaly. As line spacing decreases to 1600 m (Fig. 6b), resolution improves, with clearer geological features and reduced artefacts. At 800 m spacing, major features and linear structures become well delineated with minimal artefacts (Fig. 6c). The highest resolution is achieved at 400 m spacing, with sharply defined anomalies and minimal standard deviation values, providing the most detailed geological insights (Fig. 6d).

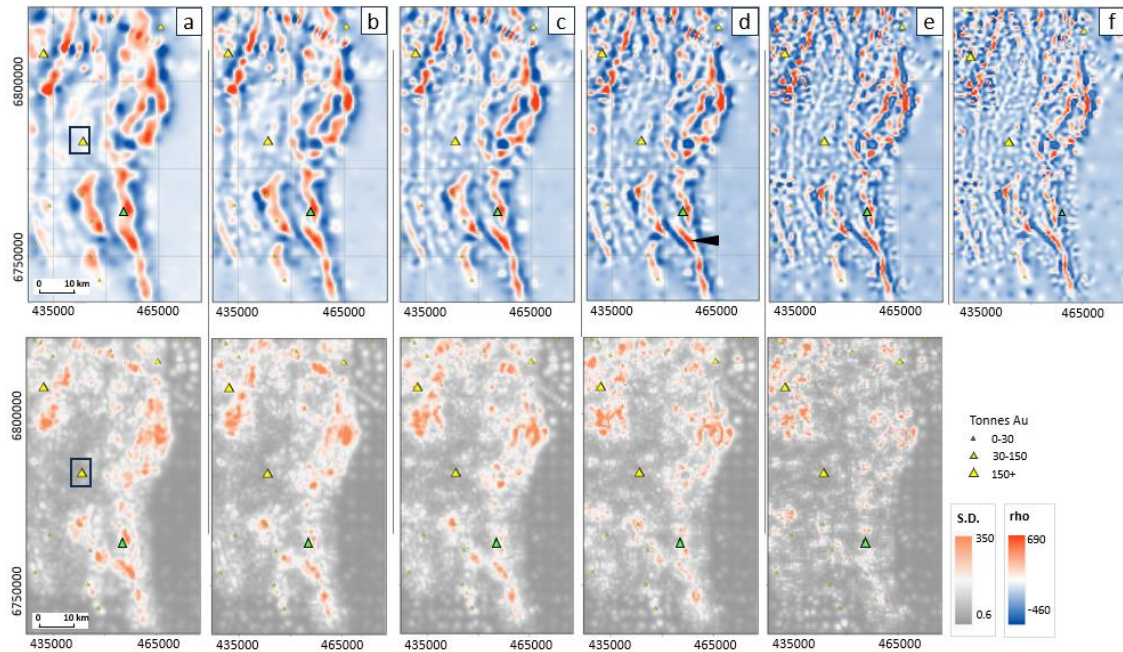


**Figure 5.** Mean (top) and standard deviation (bottom) of gravity inversion results at 1100 m depth using (a) 300; (b) 600; (c) 1000; (d) 1500; (e) 3000 points, and (f) the full dataset (3470 points). Poor gravity coverage near Sunrise Dam is marked in (a), with yellow triangles indicating gold occurrences and the green triangle marking the Fortitude North prospect. Location of maps is shown in Figure 1b.

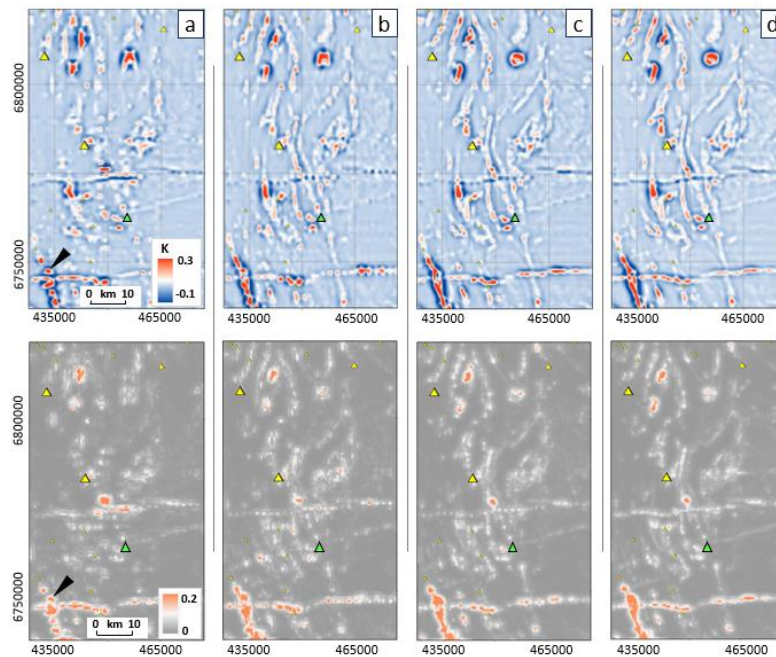


**Figure 6.** Mean (top) and standard deviation (bottom) of aeromagnetic data inversion results (K) using (a) 3200 m; (b) 1600 m; (c) 800 m; and (d) 400 m line spacing at 1100 m depth. Yellow triangles mark known deposits, and the green triangle marks the Fortitude North prospect. Location of maps is shown in Figure 1b.

### PROBABILITY APPROACH

A probability-based approach has been applied based on the cumulative distribution of density and magnetic susceptibility estimates across the study area to assess the probability of encountering specific values within the targeted ranges of density (2.8 to 3.1 g/cm<sup>3</sup>) and magnetic susceptibility (0.007 to 0.090 SI units). These specific ranges are expected for magnetite-rich dolerites (Dentith & Mudge, 2014). Along with the published bulk density and magnetic susceptibility measurements from three drill holes at the Fortitude North prospect were used to analyse the inversion results and map the spatial extent of the estimated density and magnetic susceptibility ranges of interest.

The probability map generated based on 300, 600, 1000, 1500, and 3000 measurement points inversion results were used to identify high-probability zones of density ranges 2.8 to 3.1 g/cm<sup>3</sup> and magnetic susceptibility 0.007 to 0.090 SI units (Fig. 7). The map generated with 300 measurement points displayed sparse and isolated high-probability zones, reflecting limited resolution. As the number of measurement points increased to 600 and 1000, the high-probability zones became more coherent and continuous, with improved definition of geological features. With 1500 points, the high-probability zones showed significant refinement, exhibiting clearer trends and continuity. Finally, the inversion model using 3000 measurement points exhibited the highest resolution, with highly continuous and extensive high-probability zones that accurately captured the expected density range for doleritic rocks.

For aeromagnetic data, the analysis was conducted using the inversions results from line spacings of 3200 m, 1600 m, 800 m, and 400 m. The 3200 m line spacing resulted in probability maps with diffuse, low-resolution anomalies and limited detail, as large geological features were poorly defined. At 1600 m line spacing, the probability maps showed clearer boundaries and improved resolution of larger geological trends, though still lacked finer detail. With 800 m line spacing, the resolution of geological features increased significantly, with more precise delineation of magnetic anomalies. Finally, at 400 m line spacing, the probability map exhibited the highest level of detail, capturing fine-scale features and providing highly continuous and extensive high-probability zones.

## BUFFERING AND CAPTURE EFFICIENCY ANALYSIS

Following the probability analysis of density and magnetic susceptibility estimates, techniques such as buffering and capture-efficiency (Baddeley et al., 2021; Chen & Wu, 2017; Porwal et al., 2010a) help address spatial uncertainties and evaluate the effectiveness of inversions in capturing known gold deposits. Capture-efficiency curves measure the relationship between the area fraction explored and the percentage of known gold endowment captured. A series of progressively larger buffer thresholds of 500 m, 1.0 km, 1.5 km and 2.0 km were generated around the areas with a 50% probability of presence of specific density or magnetic susceptibility values (expected ranges for magnetite-rich dolerite) for the 1100 m depth slices illustrated in Figure 7, within GIS environment.

For density estimates, the high-probability zones of 2.8 to 3.1 g/cm<sup>3</sup> range indicated that a 1.0 km buffer around high-probability zones captured 72% of the known gold endowment while covering only 42% of the total search area (Fig. 8). This buffer size was identified as the optimal threshold (Baddeley et al., 2021; Porwal et al., 2010a; Youden, 1950), balancing search area with discovery potential. Larger buffers captured more of the gold endowment but with diminishing efficiency. In the case of magnetic susceptibility estimates, a 0.5 km buffer around high-probability zones of 0.007 to 0.090 SI units range captured 92% of the gold endowment while covering only 25% of the total area.

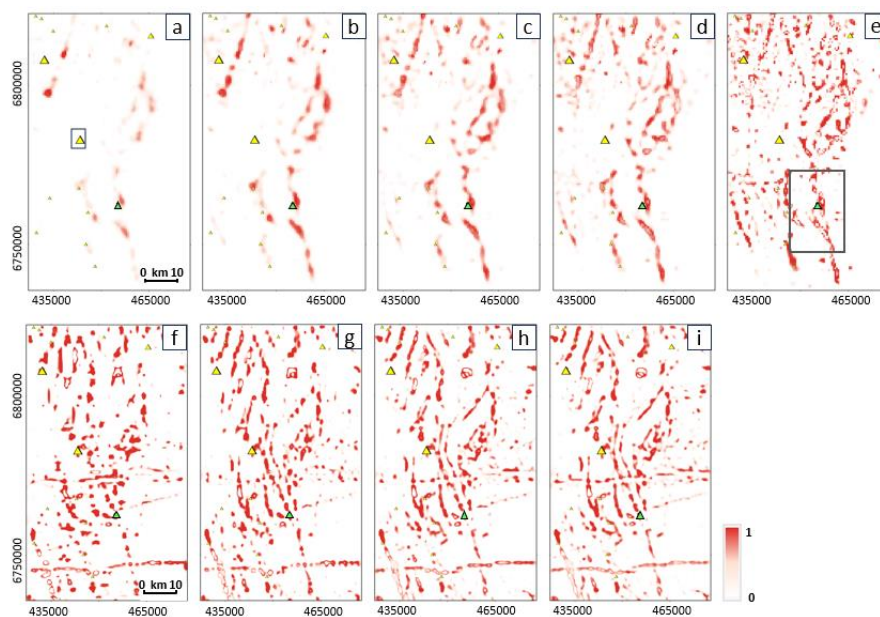


**Figure 7.** Probability maps for density estimates (2.8 to 3.1 g/cm<sup>3</sup>) from gravity inversions at 1100 m depth, using (a) 300, (b) 600, (c) 1000, (d) 1500, and (e) 3000 measurement points. The rectangle in (a) highlights poor gravity coverage near Sunrise Dam, and the rectangle in (e) shows the region used for the area reduction scenarios presented in Table 1. Probability maps for magnetic susceptibility (0.007 to 0.090 SI units) from aeromagnetic data with line spacings of (f) 3200 m, (g) 1600 m, (h) 800 m, and (i) 400 m. Yellow triangles indicate known deposits (legend shown in Fig. 1a), and the green triangle shows the Fortitude North prospect.

The intersection of optimal areas for density and magnetic susceptibility can identify more precise zones for gold mineralisation. By overlaying 1.0 km buffer for density and 500 m buffer for magnetic susceptibility, the search area is reduced to 14% while capturing ~70% of the gold endowment. Sunrise Dam was excluded from the density analysis due to poor gravity coverage, but its inclusion could potentially increase the captured endowment further.



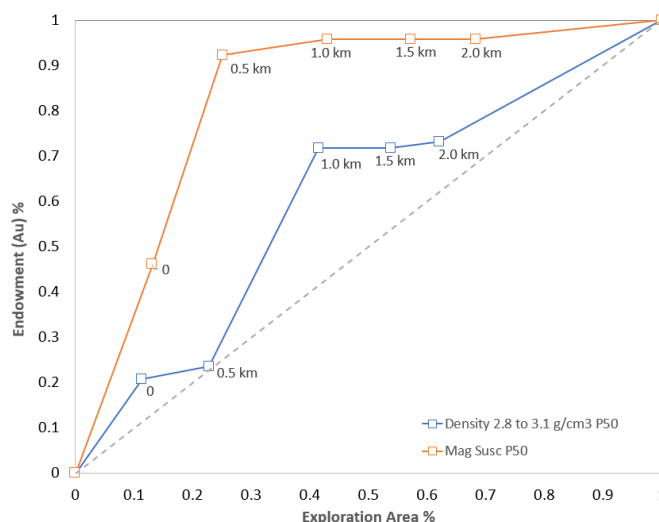


**Figure 8. Capture-efficiency curves for density and magnetic susceptibility with their associated buffers from 0.0 to 2.0 km.**

### IMPLICATIONS FOR AREA REDUCTION AND VALUE CREATION FOR EXPLORATION

Building on the results of the capture-efficiency analysis, the implication of applying these methods is a significant reduction in search area while maximising economic returns. Four scenarios were evaluated in an area of ~450 km<sup>2</sup> around the Fortitude North prospect (inset in Fig. 7e), comparable to the size of a typical mineral exploration tenement, to assess the effectiveness of different geophysical surveys, both individually and in combination, in progressively narrowing the search volume for a hypothetical 1 Moz deposit. For the purposes of these scenarios, the Net Present Value (NPV) of a 1 Moz deposit is assumed to be \$200M. However, due to the uncertainty inherent in exploration, this value has been adjusted by a risk coefficient to account for the risk of discovering such a deposit within the search area.

The risk factor is estimated based on the density of >1 Moz deposits per square kilometre within the EGS greenstone belts, where 36 deposits, each with a total contained resource >1 Moz, are located within ~61,000 km<sup>2</sup> greenstone belt area. This results in a discovery probability of 0.0006 per square kilometre. Applying this factor to a tenement size area containing ~230 km<sup>2</sup> greenstone belt (inset in Figure 7e) yields a risk coefficient of ~0.14, suggesting the area is expected to host 0.14 of a 1 Moz deposit. Consequently, the discounted NPV used in decision-making for these scenarios is ~\$27M (\$200M x 0.14). It is important to note that all cost estimates in these scenarios are illustrative examples and should not be taken as market values.

In Scenario 1, traditional drilling without any prior geophysical surveys is considered to find the 1 Moz deposit. With an assumed discounted NPV of \$27M and 250-meter drilling spacing required to adequately cover the area to locate the deposit, the total drilling cost would be ~\$370M. This far exceeds the discounted deposit's value (\$27M NPV), making the scenario economically unviable (Table 1). Scenario 2 employs gravity surveys to narrow the search area to ~47%. Drilling is then focused within the area defined by gravity anomalies. At an assumed cost of \$100 per station, the total cost of exploration data collection would be ~\$180M, which remains higher than the discounted NPV, thereby destroying value. In Scenario 3, the use of aeromagnetic surveys reduces the search area to ~28%. Drilling is then focused within the area defined by aeromagnetic anomalies. The cost of aeromagnetic data, assumed at \$15 per km, plus drilling results in a total expenditure of just over \$100M, which is still higher than the deposit's discounted NPV, rendering the scenario economically unviable. Scenario 4 combines both gravity and aeromagnetic surveys, further reducing the search area to ~19%. Drilling is then focused within the overlap of the anomalies identified by both techniques. The total exploration cost in this scenario is ~\$70M, still exceeding the deposit's discounted NPV. A potential fifth scenario involves further refinement of the search area by incorporating ground magnetic surveys in zones where favourable magnetite-bearing doleritic host rocks intersect structures. This approach, combined with 3D seismic data—estimated to cost around \$2.0M—would provide valuable insights into the dip of the dolerite and associated structures, potentially reducing the exploration area to as little as 5%. Drilling is then focused within this small area. The total cost for this highly targeted exploration strategy is estimated at ~\$21M, making it a cost-effective investment for a deposit with a discounted NPV of \$27M.

Method	Area reduction	Cost	Risk Adj. NPV
<b>Scenario 1</b>			
Drilling	100% → 0%	~\$370M	~\$343M
<b>Scenario 2</b>			
Gravity	100% → 47%	~\$45k	
Drilling	to find deposit	~\$180M	
<b>Total</b>		~\$180.05M	~\$153.05M
<b>Scenario 3</b>			
Aeromagnetic	100% → 28%	~10k	
Drilling	to find deposit	~\$100M	
<b>Total</b>		~\$100.01M	~\$73.01M
<b>Scenario 4</b>			
Gravity + Aeromagnetic	100% → 19%	~\$55k	
Drilling	to find deposit	~\$70M	
<b>Total</b>		~\$70.05M	~\$43.05M
<b>Hypothetical Scenario</b>			
Gravity + Aeromagnetic	100% → 19%	~\$55k	
Ground magnetic	19% → 5%	~\$90k	
3D seismic	5% → ?	~\$2.0M	
Drilling	to find deposit	~\$18.5M	
<b>Total</b>		~\$21M	~\$7M

**Table 1. Summary of area reduction scenarios for exploration, showing the methods, their associated costs, and the adjusted NPV based on a \$200M NPV deposit discounted to \$27M.**

## CONCLUSIONS

The use of a conceptual mineral system model provided a structured approach for interpreting complex geophysical data, identifying key geological features such as magnetite-rich dolerite hosts. The integration of potential field inversion results with geological and petrophysical data, including drill hole information from the Fortitude North prospect, further validated the geophysical models.

The results from utilising a probability-based approach in this study demonstrated a strong correlation between gold endowment and the overlay areas with density ranges of 2.8 to 3.1 g/cm<sup>3</sup> and magnetic susceptibility of 0.007 to 0.090 SI units, expected ranges for magnetite-rich dolerites. However, poor gravity coverage near Sunrise Dam excluded this major deposit from the mapped areas, underscoring the impact of data resolution on analysis.

These scenarios illustrated the significant value that can be created by employing geophysical surveys to reduce the search space, thereby lowering exploration costs, and increasing the return on investment for mineral discoveries. The methodologies outlined in this study provide a robust framework for future mineral exploration projects, offering valuable insights for ongoing research and exploration activities.

## ACKNOWLEDGMENTS

This work has been supported by the Mineral Exploration Cooperative Research Centre whose activities are funded by the Australian Government's Cooperative Research Centre Program. We gratefully acknowledge Matsa Resources for providing ground magnetic and seismic dataset as well as access to the Fortitude North geological dataset and drill core, field support and logistics. Special thanks to Camilo Guarin and Kylie Black for the help with gathering petrophysical data at the Red October core shed.

## REFERENCES

- Baddeley, A., Brown, W., Milne, R. K., Nair, G., Rakshit, S., Lawrence, T., Phatak, A., & Fu, S. C. (2021). Optimal Thresholding of Predictors in Mineral Prospectivity Analysis. *Natural Resources Research*, 30(2), 923-969.
- Blaikie, T., Ailleres, L., Betts, P., & Cas, R. (2013). Three-dimensional potential field modelling of the subsurface morphology of complex maar volcanoes - Examples from the Newer Volcanics Province, Western Victoria. *ASEG Extended Abstracts*, 2013(1), 1-4.



- Chen, Y., & Wu, W. (2017). Mapping mineral prospectivity using an extreme learning machine regression. *Ore Geology Reviews*, 80, 200-213.
- Dentith, M., & Mudge, S. T. (2014). Geophysics for the Mineral Exploration Geoscientist. *The AusIMM bulletin* /(6).
- Giraud, J., Ogarko, V., Martin, R., Jessell, M., & Lindsay, M. (2021). Structural, petrophysical and geological constraints in potential field inversion using the Tomofast-x v1.0 open-source code. *Geosci. Model Dev. Discuss.*, 2021, 1-51.
- Groves, Goldfarb, R. J., Robert, F., & Hart, C. J. (2003). Gold deposits in metamorphic belts: overview of current understanding, outstanding problems, future research, and exploration significance. *Economic Geology*, 98(1), 1-29.
- Hayman, P., Campbell, I. H., Cas, R. A., Squire, R. J., Douth, D., & Outhwaite, M. (2021). Differentiated Archean dolerites: igneous and emplacement processes that enhance prospectivity for orogenic gold. *Economic Geology*, 116(8), 1949-1980.
- Hronsky, J. M. A., & Kreuzer, O. P. (2019). Applying spatial prospectivity mapping to exploration targeting: Fundamental practical issues and suggested solutions for the future. *Ore Geology Reviews*, 107, 647-653.
- Korsch, R., & Doublier, M. (2016). Major crustal boundaries of Australia, and their significance in mineral systems targeting. *Ore Geology Reviews*, 76, 211-228.
- McCuaig, & Hronsky, J. M. (2014). The mineral system concept: the key to exploration targeting. *Society of Economic Geologists Special Publication*, 18, 153-175.
- Ogarko, V., Frankcombe, K., Liu, T., Giraud, J., Martin, R., & Jessell, M. (2024). Tomofast-x 2.0: an open-source parallel code for inversion of potential field data with topography using wavelet compression. *Geoscientific Model Development*, 17(6), 2325-2345.
- Phillips, G., Vearncombe, J., & Eshuys, E. (2019). Gold production and the importance of exploration success: Yilgarn Craton, Western Australia. *Ore Geology Reviews*, 105, 137-150.
- Phillips, G. N., Groves, D. I., & Kerrich, R. (1996). Factors in the formation of the giant Kalgoorlie gold deposit. *Ore Geology Reviews*, 10(3-6), 295-317.
- Porwal, A., Gonzalez-Alvarez, I., Markwitz, V., McCuaig, T., & Mamuse, A. (2010a). Weights-of-evidence and logistic regression modeling of magmatic nickel sulfide prospectivity in the Yilgarn Craton, Western Australia. *Ore Geology Reviews*, 38(3), 184-196.
- Youden, W. J. (1950). Index for rating diagnostic tests. *Cancer*, 3(1), 32-35.
- Yousefi, M., Carranza, E. J. M., Kreuzer, O. P., Nykänen, V., Hronsky, J. M., & Mihalasky, M. J. (2021). Data analysis methods for prospectivity modelling as applied to mineral exploration targeting: State-of-the-art and outlook. *Journal of Geochemical Exploration*, 229, 106839.